International Journal of Environment, Agriculture and Biotechnology
Vol-9, Issue-5; Sep-Oct, 2024
Peer-Reviewed International Journal
Journal Home Page Available: https://ijeab.com/
Journal DOI: 10.22161/ijeab

Analysis of Spatiotemporal Characteristics of Urban Heat Island (HUI) Effect in Shantou City based on Landsat Images

Manqi Chen, Ruei-Yuan Wang*

School of Sciences, Guangdong University of Petrochem Technology (GDUPT), Maoming 525000, China

Received: 24 Jul 2024; Received in revised form: 26 Aug 2024; Accepted: 01 Sep 2024; Available online: 07 Sep 2024

Abstract— *With the continuous strengthening of China's economic strength and the acceleration of urbanization, a series of urban ecological problems have also emerged, among which Urban Heat Island (UHI) is one of the more serious issues. This article takes Shantou City as the research object, based on Landsat series satellite images, uses the radiative transfer equation algorithm (atmospheric correction method) to invert the surface temperature of Shantou City, and uses the mean standard deviation method to classify the heat island effect of surface temperature. The results indicate that the area of UHI effect in Shantou is continuously increasing, and there is a phenomenon of transition from low-temperature areas to high-temperature areas. From 2008 to 2021, the UHI area in Shantou exhibited a spatiotemporal variation pattern of scattered, contiguous, and diffusive transfer.*

Keywords— ***Urban Heat Island (UHI); Land Surface Temperature (LST); Urban Heat Island Classification; Spatiotemporal feature analysis; Shantou City***

I. INTRODUCTION

The concept of urban heat island (UHI) was first proposed by Manley in 1958, referring to the phenomenon where the temperature in the city is significantly higher than that in the surrounding suburbs [1]. UHI is an environmental phenomenon that occurs during the process of urban economic development and is also a form of "heat pollution." [2]. With the rapid development of urbanization and industrialization and the rapid expansion of urban population, the types of urban surface cover have changed, and the quality of the atmospheric environment continues to decline. Urban water bodies, atmosphere, and surface cover have been disturbed or damaged by human activities. At the same time, the diffusion ability of the thermal environment in the city center slows down, the purification ability of the thermal environment weakens, and the heat accumulation in the city center increases while the heat in the surrounding suburbs decreases, resulting in a vicious cycle of heat transfer between the city and the suburbs[3]. The UHI effect causes a series of environmental problems, which have a serious impact on people's lives and production, such as abnormal climate and environment, warm winters, acid rain, spring sandstorms, high temperatures in summer, deteriorating air quality, and weakened air diffusion capacity.

The urban thermal environment is a unique combination of natural and man-made buildings within a city and is an important component of the urban ecosystem.

As a place where human life and production gather, cities are the most frequent places for energy and information exchange on the Earth's surface [2]. The quality of urban ecology is directly related to people's quality of life, health index, and the economic development of a country. Therefore, improving the quality of human habitation and urban environment index, adhering to the high-quality development of urban economy and ecological environment, and moving towards a sustainable green ecological path are the keys to the rational and healthy development of cities. Studying urban thermal environment can not only comprehensively understand the urban spatial structure and development scale but also guide the sustainable development of urban ecological environment, providing an important basis for improving the environmental quality of human residential areas.

Research on UHI can be divided into atmospheric heat islands and surface urban heat islands. Among them, the UHI is analyzed by establishing mathematical models or using statistical methods based on meteorological station data. In 1972, Rao first applied remote sensing technology to the study of the UHI effect [4]. Due to the advantages of good time synchronization, wide coverage, and high spatial resolution of remote sensing inversion of surface temperature data, it can display the spatial distribution of the thermal environment and compensate for the limitations of uneven distribution and low relative density of meteorological stations on UHI research [5]. With the rapid development of qualitative and quantitative remote sensing technology, remote sensing thermal infrared data has been widely used in land surface temperature (LST) inversion and UHI inspection, becoming an important tool and means that cannot be ignored [6, 7]. In addition, studies have shown that the intensity of UHIs exhibits different characteristics over time, such as strong nighttime intensity and weak daytime midday intensity. The annual variation is characterized by strong autumn and winter seasons and weak summer seasons. The intensity varies with space. For example, the heat island appears in densely populated areas with high building density and the highest concentration of industry and commerce, while the suburbs have better vegetation coverage or dense farmland, resulting in lower heat island intensity.

Based on the above, this study adopts remote sensing inversion technology, utilizes Landsat series satellite images, and uses the support vector machine (SVM) classification method for supervised classification of images. The radiative transfer equation algorithm is used to invert the surface temperature of Shantou City, and the mean standard deviation method is used to classify the heat island effect of surface temperature, focusing on the analysis of spatiotemporal characteristics. By analyzing the spatial distribution conditions and understanding the driving factors, provide a scientific basis for policy planning and improvement measures.

II. STYDY AREA AND DATA SOURCES

2.1 Study Area

The geographical location of Shantou is 116°14'40 "-117°19'35" east longitude and 23°02'33 "-23°38'50" north latitude. The total area of the city is 2064 square kilometers, with a population of 4.68 million and a coastline of 298 kilometers. Shantou City is located in the subtropical monsoon climate zone, with a mild climate throughout the year, abundant sunshine, and abundant rainfall [8]. This climate condition will to some extent promote the UHI effect. The large number of buildings, roads, population agglomeration, and other activities within the city can lead to an increase in surface temperature, making the UHI effect more significant. The administrative district governs six districts, including Jinping, Longhu, Chenghai, Haojiang, Chaoyang, and Chaonan, as well as Nan'ao County (Figure 1). Controlling the mouths of Hanjiang, Rongjiang, and Lianjiang rivers, the Tropic of Cancer spans the entire region, with winding and long coasts and spectacular hills.

Shantou City takes the secondary and tertiary industries as its main economic activity locations. A large number of factories, enterprises, transportation, and other industrial activities will release a large amount of heat, further exacerbating the formation of the urban heat island effect. In the process of urbanization, large-scale land development, cement construction, asphalt paving, and other activities will change the type and nature of surface coverage, increase the surface heat capacity, and further exacerbate the UHI effect. Meanwhile, the disappearance of large-scale green spaces and wetlands has weakened the

city's ability to regulate heat, making it more vulnerable to the impacts of climate change and human activities.

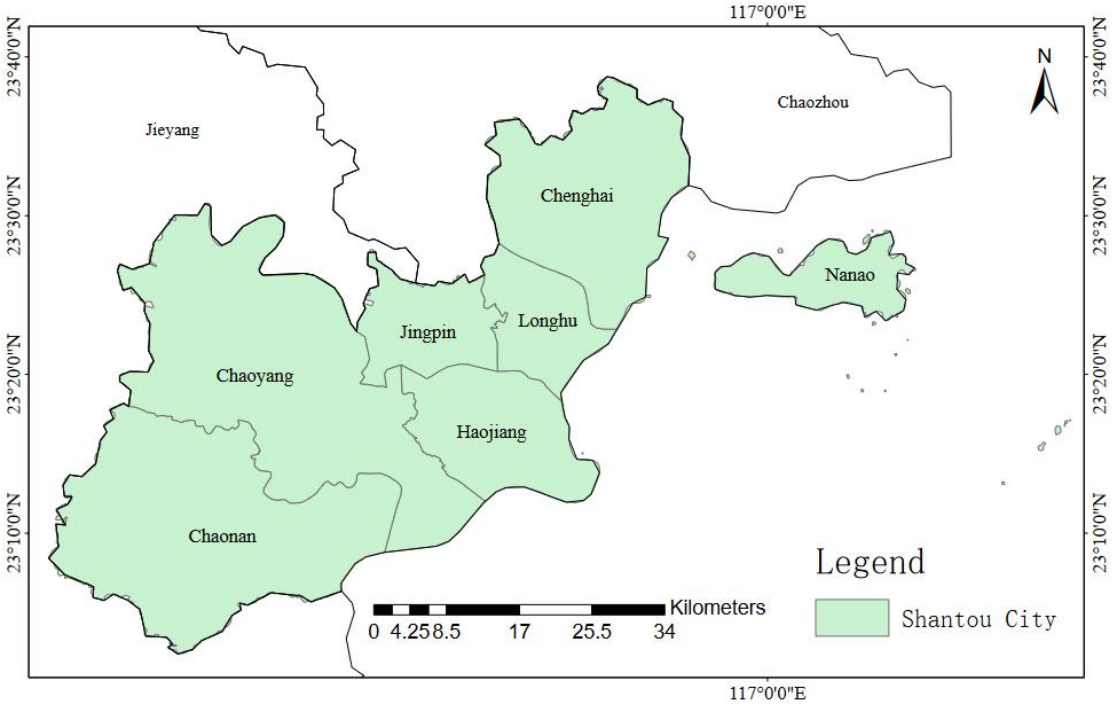

Fig.1 Administrative boundary of Shantou City

2.2 Data Sources

This article uses satellite images from the Landsat series, including Landsat-5/TM data from 2008 and monthly similar images from Landsat-8/OLI in 2013, 2016, and 2021 (Table 2). The remote sensing imagery data are all from geospatial cloud data (https://www.gscloud.cn/search). The image needs to undergo preprocessing, including radiometric calibration and atmospheric correction for each period of the image. Reuse the vector boundaries of Shantou's administrative divisions to extract the scope mask of the research area.

Table 1 Remote Sensing Image Data Sources

Item	Date	Data identification	Sensor type	Spatial resolution
Imagery	2021-2-22	LC81200442021053LGN00	Landsat8_OLI/TIRS	OLI 30m TIRS/100 m
	2016-12-9	LC81200442016344LGN01		
	2013-12-1	LC81200442013335LGN00		
	2008-12-19	LT51200442008354BJC00	Landsat5_TM	TM 30m

III. METHODOLOGY

3.1 Method

In this article, the radiative transfer equation method, also known as the atmospheric correction method, is used to invert the surface temperature of Shantou City. Its principle is to subtract the influence of atmospheric radiation on the surface radiation from the total thermal radiation received by satellite sensors and convert the remaining radiation value into the corresponding surface temperature. That is to say, the total thermal radiation received by the satellite is composed of the thermal radiation value of the atmosphere, the energy reflected by the surface to the sensor, and the energy absorbed by the surface and transmitted to the sensor through the atmosphere. The advantage of the radiative transfer equation is that it is not limited by the thermal infrared band but requires four parameters: atmospheric transmittance, atmospheric upwelling radiation value, atmospheric descending radiation value, and surface emissivity.

Based on the above principles, this study used Landsat 5 and Landsat 8 images as materials. After image preprocessing, NDVI (Normalized Difference Vegetation Index) extraction, vegetation coverage calculation, and surface radiation calculation are performed. Perform radiation calculation and temperature inversion based on the tenth wave band image. Finally, analyze the spatiotemporal changes and estimate the conclusions. The technical roadmap for the research is shown in Figure 2.

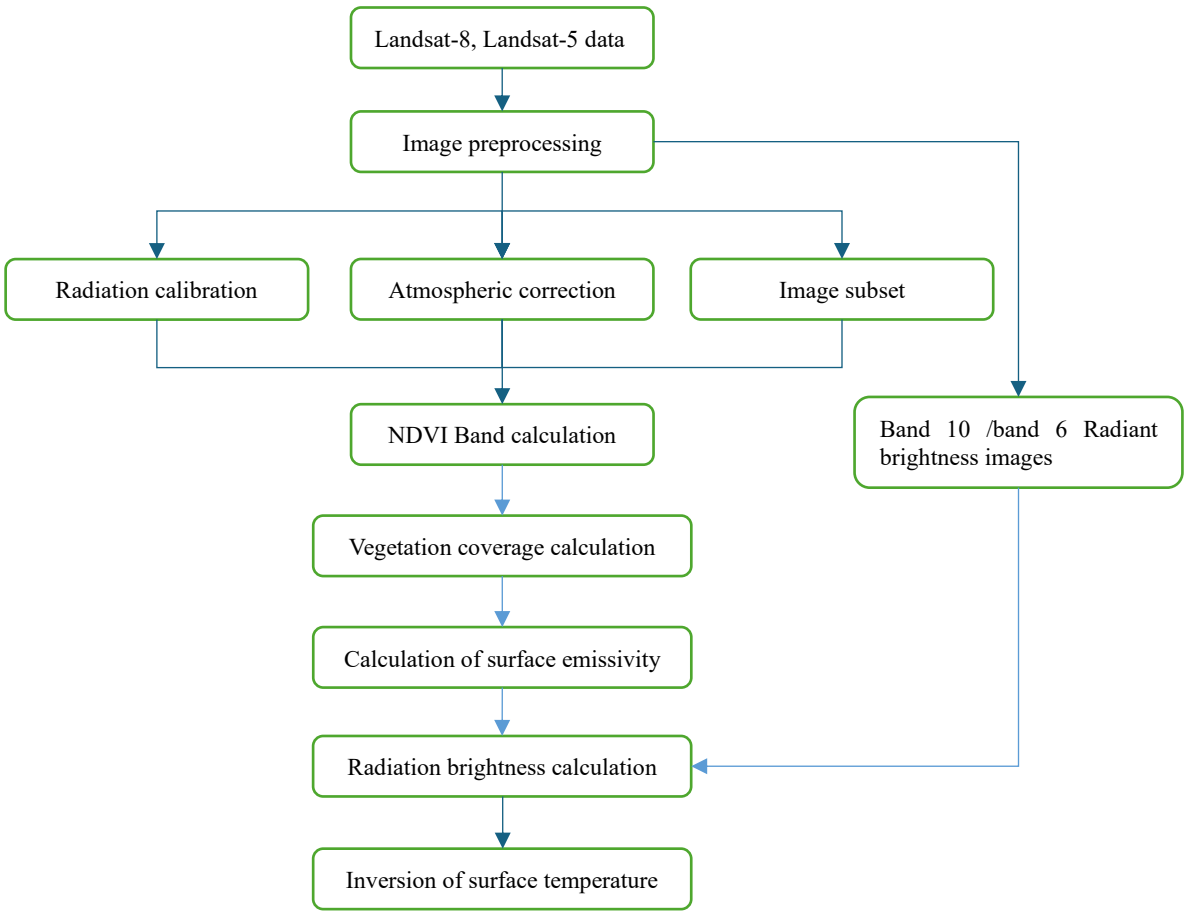

Fig.2 Technical Roadmap

3.2 Urban Surface Temperature Inversion

The physical basis for using remote sensing data to invert land surface temperature (LST) in this study is based on the heat radiation transfer equation quantified by Planck's law. According to the spectral resolution setting of satellite sensors, inversion methods are divided into single channel algorithms, dual channel algorithms (split window algorithms), and multi-channel algorithms. The temperature inversion of single channel algorithms includes the radiative transfer equation algorithm (atmospheric correction method) [9], the single window algorithm [10], the universal single channel algorithm, etc. [11]. After referring to relevant literature, this article uses the radiative transfer equation algorithm to invert temperature.

The basic principle of the radiative transfer equation algorithm is to first estimate the impact of the atmosphere on surface thermal radiation, and then subtract the atmospheric impact from the total amount of thermal radiation observed by sensors on the satellite to obtain the surface thermal radiation intensity, and then convert this thermal radiation intensity into the corresponding surface temperature. When using the radiative transfer equation algorithm for calculation, four parameters are required,

namely atmospheric transmittance, atmospheric upwelling radiation value, atmospheric downwelling radiation value, and surface emissivity. The basic calculation of the radiative transfer equation is shown in formula (1):

$$L_\lambda = [\varepsilon B(T_s) + (1-\varepsilon)L\downarrow]\tau + L\uparrow \quad (1)$$

In equation (1): Lλ is the radiance value received by the sensor, measured in W/（m2·sr·μm); ε is the surface emissivity value; B(Ts) is the radiance value of a blackbody in the thermal infrared band at the same temperature, measured in W/（m2·sr·μm）; τis the transmittance value of the atmosphere in the thermal infrared band; L↓ and L↑ are the values of atmospheric upward radiance and atmospheric downward radiance, measured in W/（m2·sr·μm）. The expression for B(Ts) is shown in formula (2):

$$B(T_s) = \frac{[L_\lambda - L\uparrow - \tau(1-\varepsilon)L\downarrow]}{\tau\varepsilon} \quad (2)$$

According to Planck's formula, the surface temperature Ts can be obtained, as shown in formula (3):

$$T_s = \frac{k_2}{\ln\left[\frac{k_1}{B(T_s)}\right] + 1} \quad (3)$$

In equation (3), K1 and K2 are both constants.

Due to different sensors, the corresponding K1 and K2 values also vary. For Band 6 of TM sensor, K1=607.76 W/（m2·sr·μm), K2=1260.56K; For Band 10 of TIRS sensor, K1=774.89 W/（m2·sr·μm), K2=774.89K.

⑵ Extraction of surface coverage index

The process of temperature inversion mainly involves the following steps: First, calculating the values of intermediate variables such as the NDVI, vegetation coverage, surface emissivity, blackbody radiance, etc. Then, substitute these intermediate values into the equation for temperature calculation. The calculation process for each parameter is as follows:

The purpose of the NDVI is to increase the reflection of vegetation in the thermal infrared band and the absorption difference of vegetation in the red band. The calculation formula is shown in equation (4):

$$M_{NDVI} = \frac{N_{NIR} - J_{Red}}{N_{NIR} + J_{Red}} \quad (4)$$

In equation (4), M_{NDVI} is the normalized vegetation index value; N_{NIR} is the reflection value of vegetation in the thermal infrared band; and J_{Red} is the value of vegetation absorption in the red band.

For different remote sensing platform sensors, their near-infrared and red bands also differ. The near-infrared band of Landsat5 is Band4, while the near-infrared band of Landsat8 is Band5. The red light bands of Landsat5 and Landsat8 are Band3 and Band4, respectively.

The vegetation coverage PV is the ratio of the projected area of vegetation on the ground to the total area. The basic calculation principle is the mixed pixel decomposition method, and the calculation formula is as follows (5):

$$P_V = \frac{M_{NDVI} - M_{NDVI_{soil}}}{M_{NDVI_{Veg}} - M_{NDVI_{soil}}} \quad (5)$$

In equation (5), $M_{NDVI_{soil}}$ is the normalized vegetation index value of bare soil or areas without vegetation cover; $M_{NDVI_{Veg}}$ is the normalized vegetation index value of pixels completely covered by vegetation, that is, the normalized vegetation index value of pure vegetation pixels. Take empirical values, $M_{NDVI_{Veg}}$=0.70, $M_{NDVI_{soil}}$=0.05; that is, when the NDVI value of a pixel is greater than 0.70, Pv is taken as 1; when the NDVI value is less than 0.05, PV is taken as 0 [12].

The surface emissivity is the ratio of the radiation emissivity of the surface to the radiation emissivity of a blackbody at the same temperature. The calculation of this value is related to the surrounding environment and the coverage type of the underlying surface. Qin et al. (2004) classified remote sensing images into three types: urban areas, water bodies, and natural surfaces. The values are calculated as follows: The specific emissivity of water body pixels is 0.995, the specific emissivity of natural surface pixels is ε surface=0.962 5+0.0614PV-0.0461PV2, and the specific emissivity of urban area pixels is ε building=0.9589+0.086PV-0.0671PV2.

The values of the atmospheric transmittance τ in the thermal infrared band, the atmospheric upward radiance value L↑, and the atmospheric downward radiance value L↓ are all obtained by searching on the website published by NASA (http://atmcorr.gsfc.nasa.gov).

3.3 Classification Method for Urban Thermal Environment Levels

UHI refers to the phenomenon where the temperature in the city is higher than that in the suburbs. However, defining the heat island area, analyzing the temperature

difference between the city and the suburbs, determining the level of thermal environment, and determining the boundaries of each level are also key issues in urban thermal environment research.

The mean standard deviation division method [13] has been widely used in UHI research. By calculating the lowest and highest temperatures obtained from inversion, the mean (u) and standard deviation (std) of the surface are obtained, and five different heat island level zones are divided into strong heat island zone, heat island zone, intermediate zone, green island zone, and cold island zone within a certain range. Li and Ren (2015) [14] used the mean standard deviation method to obtain surface temperature and classify it into different levels in the study of surface temperature inversion and quantification of UHI intensity in Xi'an. Overall, this algorithm can provide a good basis for analyzing the spatial differences of UHI; Wang (2013) [15] conducted a study on the spatiotemporal changes of the urban thermal environment in Shenyang. Based on the mean standard deviation method, the surface thermal field was divided, and the distribution pattern of the thermal environment obtained showed significant spatiotemporal resolution. Therefore, this article uses the mean standard deviation method to divide the surface temperature into five categories based on the thermal field division interval in Table 1.

Table 2 Mean-standard Deviation Temperature Classification

Heat island level	Temperature zone level	The difference in average temperature between urban core and non-core areas
Cold island	Low temperature area	$T_s < \mu - std$
Green island	Sub-low temperature area	$\mu - std \leq T_s < \mu - 0.5std$
Normal island	Middle-temperature area	$\mu - 0.5std \leq T_s < \mu + 0.5std$
Sub-heat island	Sub-high temperature area	$\mu + 0.5std \leq T_s < \mu + std$
Intense heat Island	High-temperature area	$T_s > \mu + std$

IV. ANALYSIS AND RESULTS

4.1 Distribution Characteristics of Spatiotemporal Changes in UHI

From the spatial distribution of the heat island in Shantou City (Figure 3), it can be seen that the areas of high and sub-high temperature zones have been continuously expanding from 2008 to 2021. In 2008, the heat island area was mainly distributed in the coastal and western parts of Shantou City, namely the border between Chaoyang District and Chaonan District and Longhu District, which were relatively scattered and had a small area. From 2013 to 2021, the high and sub-high temperature areas have shown an outward expansion along their original regions, mainly distributed in Chenghai District, Jinping District, and Haojiang District. The intensity of the heat island has increased at the junction of Chaoyang District and Chaonan District, as well as along the coast.

Firstly, the surface temperatures of Shantou City in 2008, 2013, 2016, and 2021 were classified using the mean standard deviation method [13] (Table 3, Figure 4, Figure 5)。 And the spatial distribution and variation trend of surface temperature were observed to exhibit the following characteristics:

1. Low temperature zone: The area of this region has significantly increased from 1.1% in 2008 to 13.99% in 2021. Although 58% of the region remains in a low-temperature state, it is worth noting that 38% of the region has transformed into a sub-low temperature zone, and 4% of the region has warmed up to a medium temperature zone, especially in the southwest of the Chaonan area and the northeast of the Chaoyang area, indicating that local areas are experiencing temperature rise.

2. Sub-low temperature zone: Between 2008 and 2016, the area of this region increased from 22.41% to 25.76%, but after reaching its peak in 2016, it sharply decreased to 8.37% in 2021. In this region, 66% of the area maintained a sub-low temperature state, while 21% of the area cooled down to the low temperature zone, 12% of the area heated up to the medium temperature zone, and 1% of the area further heated up to the sub-high temperature zone, showing complex fluctuations in temperature within the region.

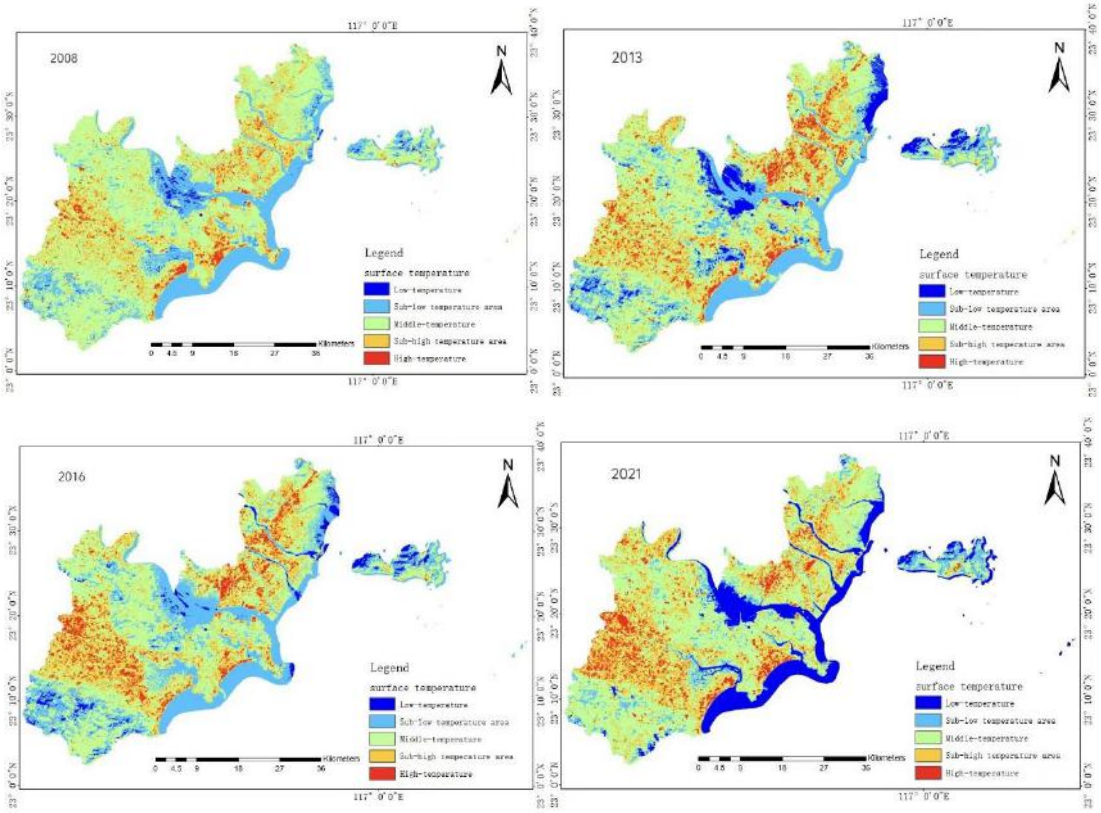

Fig.3 Classification map of Surface Temperature in Shantou from 2008 to 2021

3. Medium temperature zone: From 55.75% in 2008 to 44.18% in 2016, the area of this region shows a decreasing trend. However, from 2016 to 2021, the area of the temperate zone has rebounded, increasing to 48.51%. In this region, 70% of the area maintains a moderate temperature, 11% of the area transitions to a sub-low temperature zone, 16% of the area heats up to a sub-high temperature zone, and 1% of the area transitions to a low temperature zone and a high temperature zone, respectively, showing a polarization trend between heating and cooling in the moderate temperature zone.

4. Sub-high temperature zone: The percentage of area increased from 17.52% in 2008 to 22.27% in 2021, showing a continuous growth trend. In this region, 54% of the area remains in a sub-high temperature state, 22% of the area further heats up to the high temperature zone, and 23% of the area cools down to the medium temperature zone, indicating a coexistence of temperature rise and fall in the region.

5. High temperature zone: The area of high temperature zone increased significantly from 3.21% in 2008 to 6.18% in 2013. In this region, 50% of the area remains in a high temperature state, 34% of the area cools down to the sub-high temperature zone, 15% of the area cools down to the medium temperature zone, and 1% of the area cools down to the sub-low temperature zone, reflecting the trend of cooling in the high temperature zone while maintaining a high temperature state.

In summary, the surface temperature changes in Shantou City not only exhibit diversity in spatial distribution but also reflect the complexity of temperature dynamics within the region under the background of climate warming. Against the backdrop of global warming, temperature changes in different regions exhibit varying trends and amplitudes. The warming in some areas of the low- and sub-low-temperature regions may be due to local climate change and human activities. The warming of the medium and sub-high temperature zones may indicate that these areas are gradually transitioning towards higher temperatures. The changes in the high-temperature zone indicate that although the high-temperature zone has expanded, there are also some areas where the temperature has fallen.

Table 3 Surface Temperature Grade in Shantou from 2008 to 2021

Thermal field grade	2008		2013		2016		2021	
	Area km^2	ratio%	Area km^2	ratio%	Area km^2	ratio%	Area km^2	ratio%
Low temperature area	25.73	1.10	138.98	5.93	72.63	3.10	328.04	13.99
Sub-low temperature area	525.75	22.41	509.29	21.71	604.20	25.76	196.43	8.37
Middle-temperature area	1307.78	55.75	1085.63	46.28	1036.35	44.18	1137.96	48.51
Sub-high temperature area	410.95	17.52	466.86	19.90	478.23	20.39	522.43	22.27
High-temperature area	75.40	3.21	144.85	6.18	154.21	6.57	160.74	6.85

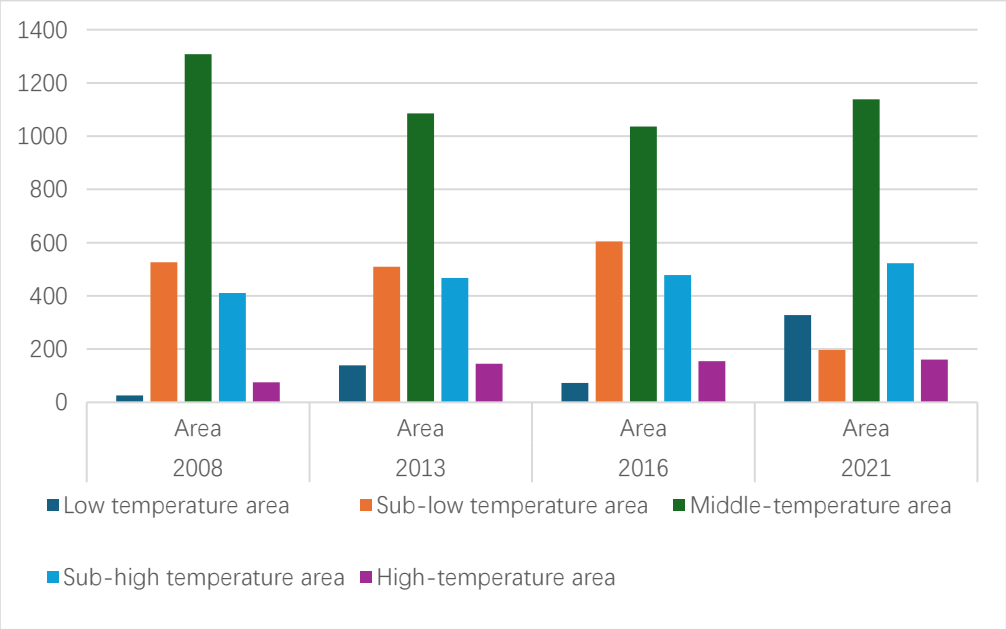

Fig.4 Map of Surface Temperature Grade Area of Shantou from 2008 to 2021

4.2 Driving Factors of UHI Evolution

This article adopts the supervised classification method in the post-classification comparison method [16] and uses the support vector machine method to classify the land use in Shantou City from 2008 to 2021 (Figure 6, Table 4) [17]. Analysis shows that from 2008 to 2021, the increase in urban built-up area and the decrease in bare land and green space are the result of a combination of multiple factors:

1. The acceleration of the urbanization process: With the development of the economy and the increase in population, the acceleration of the urbanization process has led to changes in land use patterns. In order to meet people's demand for housing, commerce, and infrastructure, a large amount of land is used for construction, resulting in an increase in building area and a decrease in bare land.

2. Economic interest-driven: Due to the scarcity of urban land resources, some local governments and developers may be more inclined to use land for profitable projects while neglecting the importance of green spaces.

3. Natural resource development: In some areas, due to natural resource development and other reasons, large areas of green space have been destroyed, resulting in a decrease in green space.

These changes have an impact on the UHI effect: an increase in building area and a decrease in green space exacerbate the UHI effect. Buildings, roads, and other

man-made structures absorb more solar energy and release heat, while reduced green spaces cannot effectively absorb heat and provide the function of regulating urban temperature, making the city hotter. The increase in bare land may also have an impact on the heat island effect. Bare land is usually prone to absorbing and storing heat, and the heat absorbed during the day is slowly released at night, causing the city's nighttime temperature to rise and further exacerbating the heat island effect.

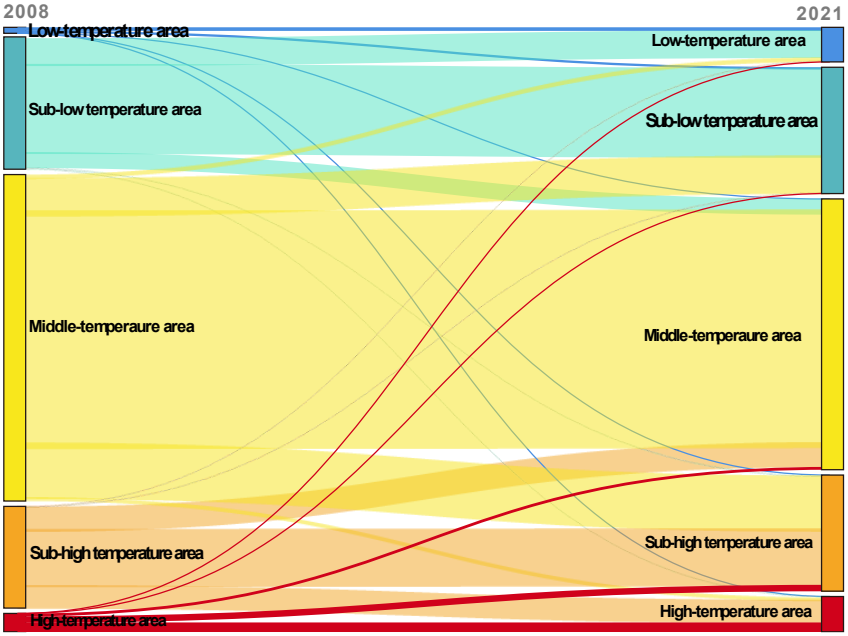

Fig.5 Temporal and Spatial Characteristics of Variation of Surface Temperature Class

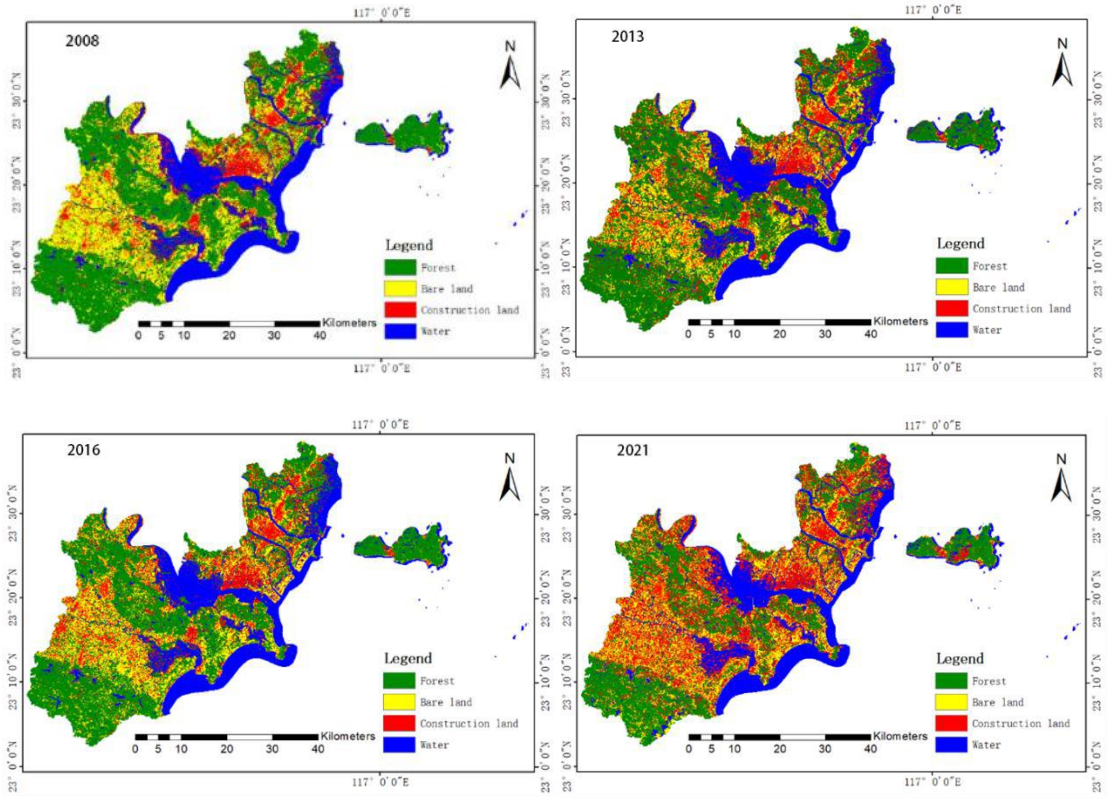

Fig.1 Land Use Classification Map of Shantou from 2008 to 2021

In summary, the increase in urban built-up area, the increase in bare land, and the decrease in green space are the result of multiple factors working together, which have a significant impact on the UHI effect and exacerbate the phenomenon of UHI effect. Thus, effective measures should be taken to plan urban development rationally, protect, and increase green spaces in order to mitigate the adverse effects of the heat island effect.

Table 4 Area and Proportion of Land Use Types in Shantou from 2008 to 2021

	2021		2016		2013		2008	
	Area km^2	ratio%	Area km^2	ratio%	Area km^2	ratio%	Area km^2	ratio%
Construction land	696.03	29.60	391.75	16.66	433.58	18.44	314.27	13.36
Bare land	450.79	19.17	465.35	19.79	394.68	16.78	528.57	22.48
Forest	710.55	30.21	989.35	42.07	1011.32	43.00	1051.29	44.70
Water	494.32	21.02	505.23	21.48	512.10	21.78	457.55	19.46

V. CONCLUSIONS

This article is based on Landsat-5 TM data from 2008, Landsat-8 OLI-TIRS data from 2013, 2016, and 2021, national basic vector data, and relevant theories of thermal environment remote sensing. Using the radiative transfer equation algorithm, the surface temperature of Shantou City in 2008, 2013, 2016, and 2021 was reconstructed, and the UHI intensity and spatial evolution pattern, as well as the thermal environment landscape pattern of Xi'an City, were analyzed. The following conclusions were drawn:

Using the atmospheric correction method to invert the spatiotemporal trend of surface temperature in 2008, 2013, 2016, and 2021. The results indicate that the overall heat island intensity in Shantou City was relatively weak in 2008, with only sporadic high-temperature areas. In 2013, the economy of Shantou City continued to develop, and the degree of greening also increased. The intensity of UHI changed from scattered to patchy distribution in the later stage, and the previous middle area has transformed into a strong heat island area or heat island area. The area of the UHI effect continues to increase with the continuous expansion of cities. In 2016 and 2021, the Green Island District in Shantou City continued to decrease, while the areas of heat island and super heat island districts increased.

⑵ In terms of the spatiotemporal characteristics of surface temperature changes, this article uses the mean and standard deviation method to divide the surface temperature of Shantou City into high temperature zones (strong heat island zone), sub-high temperature zones (heat island zone), medium temperature zones (middle zone), sub-low temperature zones (green island zone), and low temperature zones (strong green island zone). Overall, the HUI area in Shantou City has shown a trend of scattered, contiguous, and diffusive transfer from 2008 to 2021. In 2008, the scattered heat island area was distributed in the main urban area, and in 2013 and 2016, it covered the main urban area in a contiguous manner. However, in 2021, the UHI area shifted from the "urban area" to the "suburbs."

ACKNOWLEDGEMENTS

The author is grateful for the research grants given to Ruei-Yuan Wang from GDUPT Talents Recruitment (No.2019rc098), Peoples R China under Grant No.702-519208, and Academic Affairs in GDUPT for Goal Problem-Oriented Teaching Innovation and Practice Project Grant No.701-234660.

REFERENCES

[1] Manley, G. On the frequency of snowfall in metropolitan England. Quart J. Roy Meteor Soc, 1958, 84 (359): 70-72.

[2] Yu, H. Evolution of coordinated development between urbanization and eco-environment in Fujian Province. Journal of Nanchang Institute of Technology. 2011, 30 (06): 35-39.

[3] Zhou, R., Zhou, W. J., and Li, X. Y. The generation and research methods of urban heat island effect. Rural Economy and Science-Technology, 2007, (03): 113-114.

[4] Rao, P. K. Remote sensing of urban heat island from an environment satellite. Bulletin of the American Meteorological Society, 1972, 53: 647-648.

[5] Wang, J. K., Wang, K. C., and Wang, P. C. Urban Heat (or Cool) Island over Beijing from MODIS Land Surface Temperature. National Remote Sensing Bulletin, 2007, (03): 330-339.

[6] Li, B. and Wang, R.Y. The Analysis of the Spatio-temporal Evolution of the Heat Island Effect and its Influencing Factors in Huadu District, Guangzhou. International Journal of Environment Agriculture and Biotechnology (IJEAB). 2024 9 (2), 199-208. https://dx.doi.org/10.22161/ijeab.92.22

[7] Zhang, T., Wang, R.Y., Zhu, Z., and Wang, Y.S. Analysis of Urban Thermal Environment Effect by TIRS and GIS: A Case Study of Zhuhai, Guangdong, International Journal of Environment, Agriculture and Biotechnology (IJRAB). 2023, 8 (5), 87-100. https://dx.doi.org/10.22161/ijeab.85.14

[8] Huang, F. L., Cheng, G. Z., and Zhuang, M. H. Evaluation of tourist resource and plan of ecotourism for Shantou coastal wetland. Ecological Science, 2005, (01): 25-27.

[9] Hurtado, E, Vidal, A, and Caselles, V. Comparison of two atmospheric correction methods for Landsat TM thermal Band. International Journal of Remote Sensing, 1996, 17(2): 237-247.

[10] Qin, Z., Karnieli, A., and Berliner, P. A. mono-window algorithm for retrieving land surface temperature from Landsat TM data and its application to the Israel-Egypt border region. International journal of remote sensing, 2001, 22(18): 3719-3746.

[11] Tan, Z. H., Arnon, K., and Pedro, B. Mono-window Algorithm for Retrieving Land Surface Temperature from Landsat TM6data. Acta Geographica Sinica, 2001, (04):456-466.

[12] Tan, Z. H., Li, W. J., and Xu, B. The estimation of Land Surface Emissivity for Landsat TM6. Remote Sensing for Natural Resources, 2004, (03): 28-32+36-41+74.

[13] Chen, S. L. and Wang, T. X. Comparison Analyses of Equal Interval Method and Mean standard Deviation Method Used to Delimitate Urban Heat Island. Journal of Geo-information Science, 2009, 11 (02): 145-150.

[14] Li, B. Y., Ren, Z. Y., and Wang, Y. C. Urban Heat Island Quantitative Inversion and City Land Surface Temperature in Xi'an. Resources Science, 2014, 36 (12): 2631-2636.

[15] Wang, Y. Temporal and spatial changes of urban thermal environment remote sensing research in Shenyang City. Jilin University, 2013.

[16] Niu, X. Study on the influence of the Spatial Pattern of Land use on the intensity of Urban Heat Island in Baoji City Based on Landsat image. Chang'an University, 2018.

[17] Qian, J. G. and Zhang, Y. Analysis of the Influence of Land Use Type Change on Urban Heat Island Effect. Geomatics & Spatial Information Technology, 2024,47(04):1-4.